Intramolecular Hydrogen Bonding: The Case of β-Phosphorylated Nitroxide (= Aminoxyl) Radical

by **Sébastien Acerbis**[a]), **Denis Bertin**[a]), **Bernard Boutevin**[b]), **Didier Gigmes**[a]), **Patrick Lacroix-Desmazes**[b]), **Christophe Le Mercier**[a]), **Jean-François Lutz**[b]), **Sylvain R. A. Marque***[a]), **Didier Siri**[a]), and **Paul Tordo**[a])

[a]) UMR 6517 case 542, Université de Provence, Avenue Escadrille Normandie-Niemen, F-13397 Marseille Cedex 20 (fax: +33-4-91-28-87-58; e-mail: sylvain.marque@up.univ-mrs.fr)

[b]) UMR 5076, Ecole Nationale Supérieure Chimie de Montpellier 8, rue de l'école normale F-34296 Montpellier Cedex 5

Dedicated to Professor *Hanns Fischer*, deceased on February 22, 2005, for his invaluable contribution to the fields of nitroxide-mediated polymerization and radical chemistry

Alkoxyamines and persistent nitroxide (= aminoxyl) radicals are important regulators of nitroxide-mediated radical polymerization. Since polymerization times decrease with the increasing homolysis rate constant of the C–ON bond homolysis between the polymer chain and the aminooxy moiety, the factors influencing the cleavage rate constant are of considerable interest. It has already been shown that the value of the homolysis rate constant k_d is very sensitive to the stabilization of both released radical species. X-Ray, EPR, and kinetic data showed that the intramolecular H-bonding radical in the 1-(diethoxyphosphoryl)-2,2-dimethylpropyl 2-hydroxy-1,1-dimethylethyl nitroxide (**3a**) (homologue of 2-hydroxy-1,1-dimethylethyl 1-phenyl-2-methylpropyl nitroxide (**2a**)) did not occur with the nitroxide moiety as expected but with the phosphoryl group. However, the polymerization rate of styrene (= ethenylbenzene) was significantly enhanced.

Introduction. – Two decades ago, *Rizzardo* and co-workers [1] and *Georges* and co-workers [2] showed that it was possible to prepare well-defined polymers by using nitroxide (= aminoxyl) radicals or alkoxyamines as controllers. The nitroxide-mediated polymerization (NMP) was born [3], and numerous studies have been undertaken to elucidate the mechanism [4] and the kinetics of the polymerization [5], to prepare new polymers [3][6], and to develop more efficient initiators/controllers [7]. *Scheme 1* displays the simplified NMP process [8] where k_d is the rate constant of C–ON bond homolysis in the alkoxyamine (so-called dormant species), k_c the rate constant for the reformation of the alkoxyamine, k_t the rate constant of self-termination, and k_p the propagation rate constant of the polymerization.

Alkoxyamines ($R^1R^2NOR^3$) are key intermediates [4] of the NMP process, and the strength of the C–ON bond is a crucial parameter to control [4][5][7a,h,i]. It has been shown that the activation energy (E_a) of the homolysis is a good approximate of the value of the bond-dissociation energy (*BDE*) of the C–ON bond of alkoxyamines [9]. We [7e][9a][10] and others [7a][11] have shown that the C–ON bond of alkoxyamines was either strengthened by hyperconjugation [11c,f] (heteroatom bonded to the C-atom) and polar [7a][10d][11f,g] (electron-withdrawing (EWG) groups bonded to

Scheme 1. *Simplified Scheme of Nitroxide-Mediated Polymerization* (NMP)

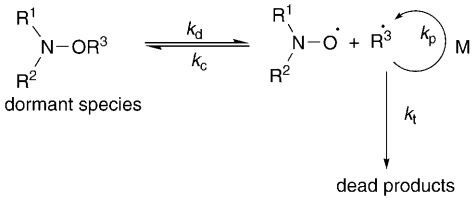

the N-atom) effects, or weakened by the stabilization [7a][9a][10a–c][11a–c,f] of the released alkyl and nitroxide [11f] (intramolecular H-bonding) radicals and by the steric strain and polar effects of both alkyl and nitroxide fragments [7a][7d–i][9][10][11]. Recently, *Hawker* and co-workers [12], carrying out a faster styrene (=ethenylbenzene) polymerization with nitroxide radical **1a** than with nitroxide radical **2a** (*Fig. 1*), exemplified the importance of the intramolecular H-bonding on the nitroxide moiety.

It prompted us to study the X-ray, electron paramagnetic resonance (EPR), kinetic, and polymerization properties of the nitroxide radical **3a** (*Fig. 1*), capable of intramolecular H-bonding and based on the structure of **4a** (one of the most potent and versatile nitroxide radicals for NMP).

Results and Discussion. – *X-Ray Data.* We prepared nitroxide radical **3a** with the hope that intramolecular H-bonding would increase the polymerization rate constant as already observed with **1a** and **2a** (*vide infra*). The crystals of **3a** were obtained as two separated enantiomers (*Fig. 2* and *Table 1*) under the form of an orthorhombic symmetry group cell[1]), the deracemization occurring because of the intramolecular H-bond.

Significant X-ray data such as bond lengths, interatomic distances, and bond and torsion angles of (*R*)- and (*S*)-**3a** and **4a**′ as well as significant *van der Waals* radii [13] are given in *Table 1*. Unfortunately, certainly due to this intramolecular H-bond and to the poor quality of the crystal (several attempts to prepare crystals of better quality were unsuccessful), X-ray data suffer a loss of accuracy (*ca.* 0.05 Å) and some discrepancies (see *Exper. Part*)[2]). Otherwise, bond lengths are in the range expected from the literature data [14].

A few studies showed that the N–O moiety was capable of intramolecular H-bonding (*Fig. 3*) [11f][12][15], but the *d*(O···H) between the N–O and H–O moieties of (*R*)- and (*S*)-**3a** (3.07 Å and 3.00 Å, resp., *Table 1*) were longer than the *van der*

---

[1]) CCDC-276874 contains the supplementary crystallographic data for this paper. These data can be obtained free of charge *via* http://www.ccdc.cam.ac.uk/data_request/cif from the *Cambridge Crystallographic Data Centre.*

[2]) Mainly, a too long (1.58 Å) or a too short (1.25 Å) P=O bond for (*R*)- and (*S*)-**3a**, respectively, and a too long (1.56 Å) and a too short (1.41 Å) C–N bond were noted in (*R*)-**3**.

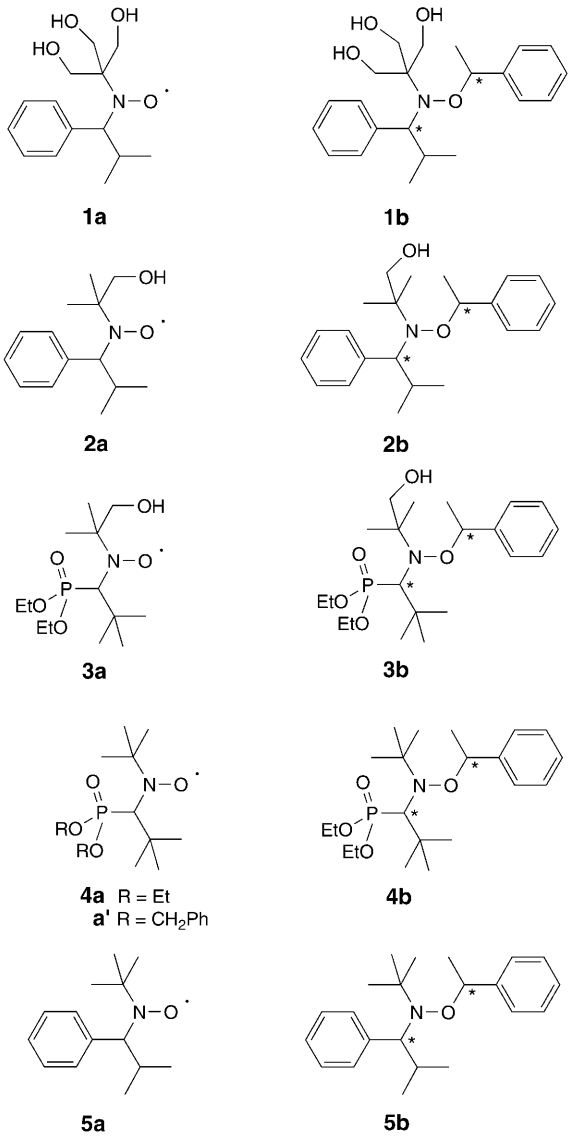

Fig. 1. *Nitroxide radicals* **1a**–**5a** *and their homologue alkoxyamines* **1b**–**5b**

Waals radii sums[3]) and the O_N-H-O_C angles were much smaller (*ca.* 108° and 113°, resp., *Table 1*) than the 180° angle generally accepted for strong intramolecular H-bonds [16]. However, these distances $d(O\cdots H)$ were smaller than 3.5 Å, and the

[3]) Although $d(N\cdots H)$ distances of both enantiomers were close to the *van der Waals* radii sums, that possibility was disregarded because the corresponding N–H–O bond angle values (*ca.* 100°) were close to 90°.

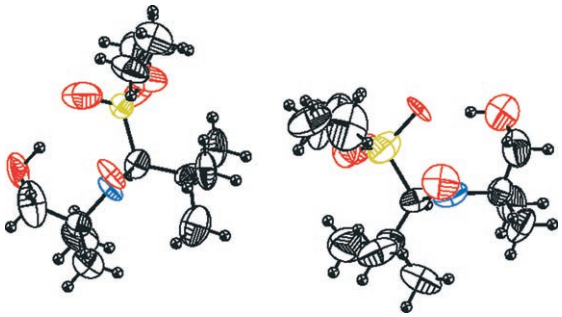

Fig. 2. *X-Ray structures of* (R)-**3a** (left) *and* (S)-**3a** (right). O-Atoms red, N-atom blue, and P-atom yellow.

Table 1. *Significant X-Ray Distances* d *[Å], Bond Lengths* l *[Å], Bond Angles [°], and Torsion Angles [°] for Nitroxide Radicals* (R)*- and* (S)-**3a** *and* **4a**′[a])

		(*R*)-**3a**	(*S*)-**3a**	**4a**′[b])	*v.d.W.* data[c])[d])	
Distances *d*:	$O_P\cdots H$	1.570	2.040	–	*v.d.W.* radii:	H 1.20
	$O_N\cdots H$	3.070	3.000	–		P 1.80
	$O_P\cdots N$	2.848(14)	3.030(15)	3.536		N 1.55
	$O_C\cdots N$	3.059(19)	2.977(13)	–		O 1.52
	$P\cdots O_N$	2.887(11)	2.966(8)	2.926		
	$O_C\cdots P$	3.738(14)	3.703(9)	–		
	$O_C\cdots O_P$	2.526	2.990	–		
	$H\cdots N$	2.698	2.584	–	*v.d.W.* radii sums:	OO 3.04
						OH 2.72
						ON 3.07
Bond lengths *l*:	N–O	1.294(13)	1.287(10)	1.278		OP 3.32
	O–C	1.460(20)	1.360(20)			NH 2.75
Bond angles:	O_P–H–O_C	178.1	170.2		Bond lengths[d]):	*l*(C–O) 1.426
	O_N–H–O_C	107.8	113.2			*l*(N–O) 1.463
	O_N–H–O_P	73.7	75.4			
Torsion angles:	θ_P	36.1(13)	37.4(11)	39.7		
	θ_H	81.0	80.9	77.5		
	θ_{NCPO}	39.0(9)	38.7(9)	89.3		

[a]) The errors are given in parenthesis on the last digits. [b]) From [14]. [c]) *van der Waals* (*v.d.W.*) radii are given in Å. [d]) From [13].

O_N–H–O_C, O_N–H–O_P, and O_P–H–O_C angle sum was very close to 360° for both enantiomers (359.7° and 359.8°), which are typical values of weak intramolecular H-bonds, that is, a weak $OH\cdots{}^{-}ON^{+}$ bond [17]. On the other hand, the *d*(O···H) and *d*(O···O) distances between the P=O bond and the OH group for both enantiomers (1.57 and 2.04 Å, and 2.526 and 2.990 Å, resp., *Fig. 2* and *Table 1*) were clearly and unambiguously smaller than the *van der Waals* radii sums of the OH and OO atoms (2.72 and 3.04 Å, resp., *Table 1*). Furthermore, the O_P–H–O_C angle values of (*R*)-**3a** (178.1°) and (*S*)-**3a** (170.2°) were close to 180° and thus confirmed the presence of the strong P=O···HO intramolecular H-bond. To substantiate our experimental

results, DFT calculations were performed with (*R*)-**3a**. The calculated distances differ less than 0.3 Å from those given in *Table 1* (except for $d(O_C\cdots N) = 3.682$ Å[4]), and therefore confirm the strong intramolecular H-bond between the P=O and OH functions, and the weak intramolecular H-bond between the OH and nitroxide functions. Although the calculated angle O_P-H-O_C is slightly more bent (167.1°) than the one given by the X-ray data, it confirms the strong intramolecular H-bond. The other angles are different of less than 6°. Furthermore, natural-bond-orbitals analysis shows donation ($n_{OP} \rightarrow \sigma^*_{O-H}$) of the two lone pairs (n) of the O_P atom into the anti-bonding σ^* orbital of the O–H bond, and the stabilization energy is *ca.* 56.0 kJ/mol[4]).

As can be seen from *Fig. 2*, the N–O moieties of (*R*)- and (*S*)-**3a** are much encumbered, and the P=O function is turned toward the N-atom, in contrast to what is observed for **4a**′. Identical $P\cdots O_N$ bond distances for (*R*)- and (*S*)-**3a** and **4a**′ discard a potential stabilizing electrostatic interaction between the P-atom and the O-atom of the nitroxide moiety. However, in both enantiomers of **3a**, the distances ($O_p^{\delta-}\cdots N^{\delta+}$) between the partially negatively charged O-atom of the phosphoryl group and the partially positively charged N-atom of the nitroxide moiety (due to the presence of mesomeric form **B**, see *Scheme 2*) are equal to or smaller than the *van der Waals* radii sums and shorter than that of **4a**′ (*Table 1*). Therefore, it is likely that a stabilizing electrostatic interaction occurs between the O- and N-atoms, which favors the mesomeric form **B** of (*R*)- and (*S*)-**3a** (*Fig. 3*)[5]). Moreover, the presence of that interaction is highlighted by the important changes in the N–C–P–O torsion angle from *ca.* 89° for **4a**′ to roughly 39° for (*R*)- and (*S*)-**3a** (*Table 1*). Other torsion angles, θ_P and θ_H, of (*R*)- and (*S*)-**3a** exhibit values close to those of **4a**′.

Scheme 2. *Mesomeric Forms* **A** *and* **B** *for the Nitroxide Radical*

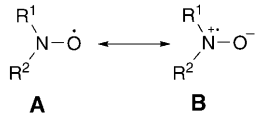

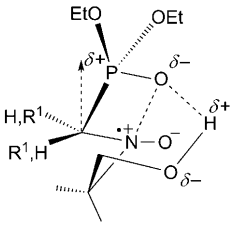

Fig. 3. *Stabilizing electrostatic interaction and intramolecular H-bonding in (*R*)- and (*S*)-***3a***

---

[4]) Supplementary material concerning the calculations is available upon request from the authors.

[5]) $d(O_C\cdots N)$ distances are close to the value of the *van der Waals* radii sums and then might possibly stabilize mesomeric form **B** (*Scheme 2*) by electrostatic interaction between the partially negatively charged O-atom of the OH group and the partially positively charged N-atom of the nitroxide moiety. Charges calculation with the CHelpG scheme [18] provided positive charges on P (+0.91), N (+0.19), and H_O (+0.42), and negative charges on O_P (−0.61), O_N (−0.42), and O_H (−0.72), as expected.

EPR Measurements. It is well established that the N-hyperfine coupling constant a_N of nitroxide radicals is sensitive to the electron-donating (ED) or electron-withdrawing (EW) capacities of the groups attached to the N–O moiety [15]. This influence can be explained on the basis of the canonical forms **A** and **B** of the nitroxide function (*Scheme 2*) [19]. ED groups will favor the form **B** more while EW groups will favor more the form **A**. Then, a_N should be larger for **B** than for **A**. Therefore, any intramolecular H-bond (*Fig. 4*) should stabilize **B** and one should observe a larger value of a_N [15]. However, *Marque* and co-workers [11f] showed that the stabilizing effect of the intramolecular H-bond might be balanced by the destabilizing effect of the EW CH_2OH group like for radicals **1a** and **2a** (*Fig. 1*, *Table 2*). Furthermore, with **1a**, **2a**, and **5a** they pointed out that the β-H hyperfine coupling constant $a_{H\beta}$ was not modified by the presence of the intramolecular H-bond when the OH group was located on the *t*Bu-like group (*Table 2*, *Figs. 1* and *4*) [11f].

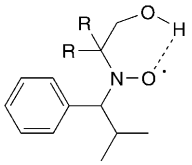

1a R = CH_2OH
2a R = Me

Fig. 4 *Typical intramolecular H-Bond in nitroxide radicals* **1a** *and* **2a**

Table 2. *EPR Data for Nitroxide Radicals* **1a**–**5a**[a])

	a_N [G]	$a_{H\beta}$ [G]	$a_{P\beta}$ [G]	Ref.
1a	14.88	2.69	–[b])	[11f]
2a	14.84	2.72	–[b])	[11f]
3a[c])	13.70	*ca.* 0[d])	40.7	this work
4a[e])	13.60	*ca.* 0[d])	46.6	this work
5a	14.83	2.66	–[b])	[11f]

[a]) In (*tert*-butyl)benzene, 10^{-4} M at room temperature. [b]) No P-atom. [c]) $g = 2.0063$. [d]) Not resolved, see text. [e]) $g = 2.0061$. **4a**′ exhibits the same EPR data, see [22].

The β-H hyperfine coupling constants a_H of both **3a** and **4a** are not resolved because the H-atom lies nearly in the nodal plan of the 3-electrons π-bond of the nitroxide moiety (*Fig. 5*), and $a_{H\beta}$ (**3a**) is not sensitive to intramolecular H-bonding, as was expected (*Fig. 6*). Similarly, the difference between a_N (**3a**) and a_N (**4a**) is not striking (*Fig. 6* and *Table 2*), as expected from a_N values of OH derivatives **1a** and **2a**. *A contrario*, the value of the β-P hyperfine coupling constant $a_{P\beta}$ of **3a** is clearly and unexpectedly much smaller than that of **4a**. In fact, this observation is very well accounted for by an intramolecular H-bond between the phosphoryl and the OH groups, as deduced from X-ray data (*vide supra*) and depicted in *Figs. 2* and *5*[6]).

Indeed, assuming $\rho_N \cdot B_P = 58$ G ($\rho_N \cdot B_X$ is the hyperconjugation term given for a family of radicals) [20] and applying the *Heller-McConnell* relationship (*Eqn. 1*) [21],

[6]) EPR hyperfine coupling constants were calculated at the level UB3LYP/6-31++G(d,p) and were close to the experimental ones, *i.e.*, $a_N = 11.8$ G, $a_H = 0.8$ G, and $a_P = 38.9$ G.

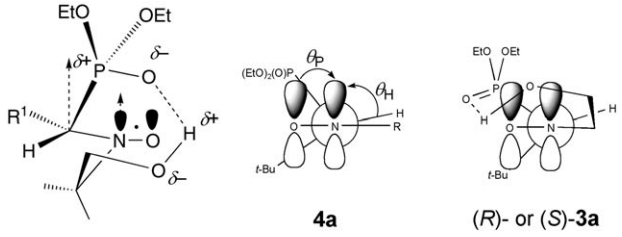

Fig. 5. Newman *projections of the intramolecular H-bonding in (*R*)- and (*S*)-***3a***

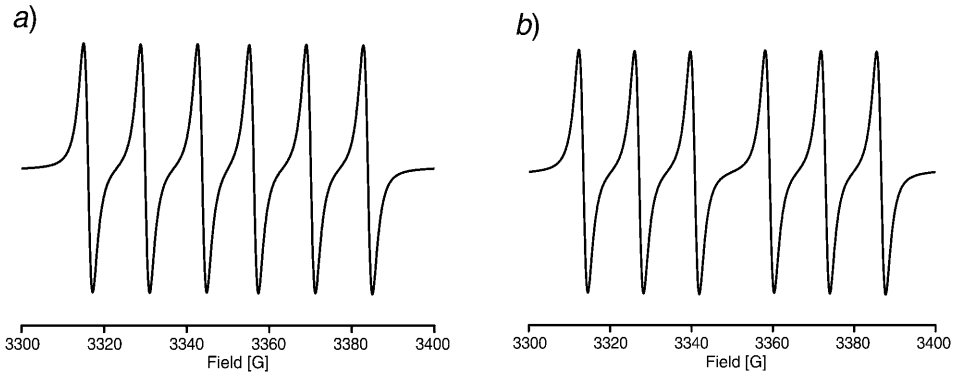

Fig. 6. *ESR spectra in (*tert*-butyl)benzene:* a*) nitroxide radical* **3a** *and* b*) nitroxide radical* **4a**

θ_P of **3a** and θ_P of **4a** (dihedral angles between the P–C–N plane and the CN orbital π plane containing the odd electron) were estimated at *ca.* 33° and 26°, respectively. The value of θ_P (**3a**) was close to the value obtained from X-ray data (see *Table 1*). Thus, by using the value of 81° given by the X-ray data (*Table 1*) for the dihedral angle θ_H (**3a**), assuming a θ_H (**4a**) of $-86°$ ($-60° - \theta_P$) and $\rho_N \cdot B_H = 26$ G [20], $a_{H\beta}$ (**3a**) and $a_{H\beta}$ (**4a**) were estimated at *ca.* 0.6 G and 0.13 G, respectively, too small to be resolved under our experimental conditions ($\Delta H_{pp} \approx 1$ G). Unfortunately, the $a_{P\beta}$ value of 32 G estimated with *Eqn. 1* ($\theta_P = 40°$ given by the X-ray structure) did not agree with the experimental EPR value of *ca.* 46 G for **4a**′ [22]. Furthermore, the X-ray value of θ_H (77.5°, *Table 1*) is sufficiently large that the $a_{H\beta}$ would have been detected. The strong difference in θ_P (**4a**′) between the X-ray data and the value deduced from the EPR liquid-phase measurements (θ_P (**4a**′) $\approx 26°$) was likely due to a crystallization (packing) effect involving a slightly different conformation in the crystal state than in solution.

$$a_{X\beta} \approx \rho_N \cdot B_X \cdot \cos^2 \theta_X \quad (1)$$

An intramolecular H-bond between the phosphoryl and the OH group suppressed the compensation of the electron-attracting effect of the OH groups, but the expected decrease in a_N (**3a**) was not observed. Indeed, the short P=O···N distances involved an electrostatic stabilization of the mesomeric form **B** and thus the electron-withdrawing effect of the OH group was balanced (*Figs. 4–6*). It is worthy to mention that the decay

of **3a** was monitored [9a] at 120° by EPR[7]) involving that the intramolecular H-bonding is detected at such high temperature and, then, is likely to occur in the course of the polymerization.

Polymerization Experiments. In the previous sections, we clearly established the presence of strong P=O···HO and weak OH···$^{-}$ON$^{+\bullet}$ intramolecular H-bonds, and of electrostatic interactions. Because the intramolecular H-bonding did not occur with the nitroxide moiety, one might expect that such H-bondings occur also in the alkoxyamine. If such a H-bonding occurs both in the transition state (TS) and in the initial state of **3b**, and assuming that the strength is the same in both states, the intramolecular H-bonding should not influence k_d. Consequently, the difference observed would be due to the combined effects of the weak intramolecular H-bond and electrostatic interactions stabilizing the TS. Such interactions occur due to the strong P=O···HO H-bond which forces the substituents to adopt the conformation depicted in *Figs. 2*, *3*, and *5*. However, the very high steric hindrance around the aminooxy moiety should disrupt the intramolecular H-bonding[8]) in the alkoxyamine [23]. Whenever there is an intramolecular H-bond (very unlikely) [23] or not in **3b**, the discussion below rests on the increase of k_d due to all the interactions observed in **3a**.

In this section, we analyze the influence of the interactions observed in **3a** in the NMP process by comparing the k_d values and the polymerization characteristics $\ln([M]_0/[M])$ *vs.* $t^{2/3}$ and average molar mass in number M_n *vs.* conversion of **3b** and those of the most efficient alkoxyamines, *i.e.*, **1b**, **2b**, **4b**, and **5b**. *Tordo* and co-workers [7b] and *Hawker* and co-workers [7c] showed that **5a** was a versatile and efficient nitroxide radical for the polymerization of styrene and a few other monomers. Recently, *Hawker* and co-workers [7c][12] applied successfully alkoxyamines **1b** and **2b** to the polymerization of styrene (3–4 h for 50% conversion and a polydispersity index *PDI* of *ca.* 1.1 at 125°, and 48 h for 50% conversion and a *PDI* of *ca.* 1.20 at 85° both for **1b**), but the decrease in the polymerization time was less striking when **2b** was used [7c]. *Hawker* and co-workers ascribed this improvement to a faster homolysis rate [12]. The two-fold increase in k_d from **5b** and **2b** to **1b** undoubtedly accounts for the shortening of the polymerization time. The 4-fold increase in k_d of **4b** to **3b** is also in good agreement with an intramolecular H-bonding, and with the electrostatic stabilizing interaction as depicted in *Figs. 3* and *5*.

A linear plot of $\ln([M]_0/[M])$ *vs.* $t^{2/3}$ (*Fig. 7*) establishes that **3b**, **4b**, and **5b** control the polymerization of styrene *via* the persistent radical effect [5]. One should note that the polymerization time decreases as k_d increases along the series **5b** < **4b** < **3b** as expected from *Eqn. 2*, where $t_{90\%}$ is the time needed to reach 90% of conversion and $[I]_0$ the initial concentration of the initiating alkoxyamine) [5][24].

$$t_{90\%} = \left(\frac{2\ln 10}{3k_p}\right)^{3/2}\left(\frac{3k_c k_t}{k_d[I]_0}\right)^{1/2} \quad (2)$$

---

[7]) At 120° in (*tert*-butyl)benzene, $a_P = 42.5$ G and $a_N = 14.0$ G for **3a**. a_P is larger than at room temperature (*Table 2*) but clearly smaller than a_P of **4a**.

[8]) Recently, crystals of **3b** were grown, and an intermolecular H-bond P=O···HO was observed and no intramolecular one.

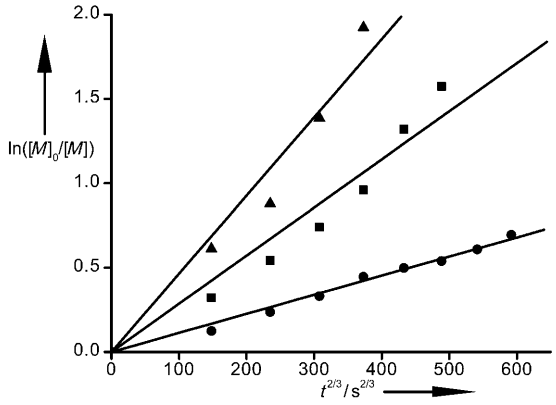

Fig. 7. *Plot of ln([M]$_0$/[M]) vs. t$^{2/3}$ for alkoxyamines* **3b** (▲), **4b** (■), *and* **5b** (●). Conditions: 200 equiv. of styrene and [alkoxyamine]$_0$ = 0.044M at 123°.

Moreover, the closeness of the polystyrene's M_n experimental values to the ideal values (bold line in *Fig. 8*) highlights the efficiency of **3b**, **4b**, and **5b** as controller agents for NMP. Thus, at $t_{50\%}$, and assuming that the chain length had no significant influence on k_d [26], the values of K and k_c were roughly estimated for polystyryl–macroalkoxyamines **1a–PS**, **2a–PS**, **3a–PS**, **4a–PS**, and **5a–PS** (*Table 3*). Hence, as expected from the close values of k_d, there is no significant difference in K between **5a–PS** and **2a–PS**, *i.e.*, the intramolecular-H-bonding effect is balanced by the EW-group effect of the OH group in **2a**. Moreover, the much more efficient intramolecular H-bonding in **1a** leads to a higher K and thus a shorter polymerization time. Although **1b** and **4b** exhibit very close k_d, the *ca.* 6 times higher value of K for **4a–PS** than for **1a–PS** well accounts for the faster polymerization observed for **4a–PS** than for **1a–PS**, and the slightly poorer *PDI* of **4a–PS**, that is, k_c of **4a–PS** is smaller than k_c of **1a–PS**. The *ca.* 4-fold, 30-fold, and 23-fold increase in K from **4a–PS** to **3a–PS**, from **2a–PS** and **5a–PS** to **3a–PS**, and from **1a–PS** to **3a–PS**, respectively (*Table 3*), highlights the importance of the intramolecular H-bonding effect on the fate of the polymerization, that is, a polymerization time *ca.* 2 times, *ca.* 5 times, and *ca.* 4.5 times shorter is observed with **3a–PS** than with **4a–PS**, **2a–PS** and **5a–PS**, and **1a–PS**, respectively, the *PDI* (<1.3) being kept low. As expected from the work of *Fischer* and co-workers [27] on the recombination of the molecular parent species (at 297 K in (*tert*-butyl)benzene, k_c(**3b**) = $3.0 \cdot 10^6$ l mol^{-1} s^{-1}, k_c(**4b**) = $3.1 \cdot 10^6$ l mol^{-1} s^{-1}, k_c(**5b**) = $8.0 \cdot 10^6$ l mol^{-1} s^{-1}), the k_c of the macromolecular species **5a–PS** is larger than those of **3a–PS** and of **4a–PS**. Furthermore, as for the molecular species **3b** and **4b**, **3a–PS** and **4a–PS** exhibit very close k_c values, which means that the intramolecular H-bonding has no effect on the recombination reaction and thus the (macro)alkyl radical approach to the nitroxide moiety is probably the same for both **3a** and **4a**. Because of the probable large experimental errors, the complicated role [28] of the H-bonding between the OH group and the nitroxide moiety in **1a–PS**, **2a–PS**, and **5a–PS** is not discussed. It is gratifying to note that the estimated value of k_c for **4a–PS** is of the same order of magnitude as the values recently measured

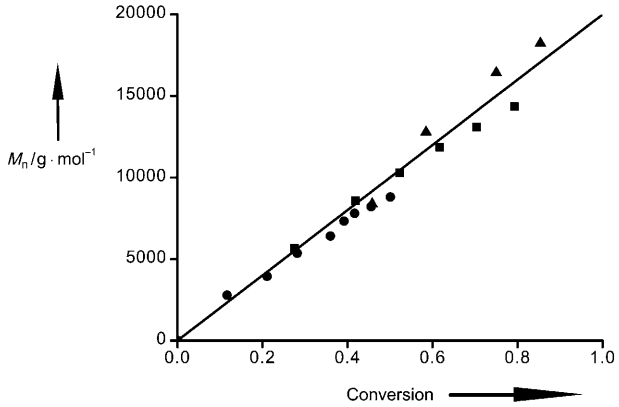

Fig. 8. *Plot of* M_n vs. *conversion for alkoxyamines* **3b** (▲), **4b** (■) *and* **5b** (●). The bold line represents the theoretical values of M_n for a truly living polymerization. Conditions: 200 equiv. of styrene and $[\text{alkoxyamine}]_0 = 0.044$M at 123°.

Table 3. *Polymerization Temperatures* T, *50% Conversion Times* $t_{50\%}$, *Averaged Number Molecular Masses* M_n *at 50% conversion, Polydispersity Indexes* PDI, *Quasi-Equilibrium Constants* K, *C–ON Bond Homolysis Rate Constants* k_d, *and Recombination Rate Constants* k_c *for the Alkoxyamines* **1b**–**5b** *and Their Polystyryl Parent Alkoxyamines*

Initiator	T [°C]	$t_{50\%}$ [h]	M_n [g·mol^{-1}]	*PDI*	K[a]) [10^{-9} mol l^{-1}]	k_d [10^{-3} s^{-1}]	k_c[b]) [10^6 l mol^{-1} s^{-1}]
1b[c])	125	*ca.* 3.5	–[d])	*ca.* 1.1	1.0	9.1[e])	8.6
2b[f])	123	*ca.* 4	*ca.* 10000	*ca.* 1.1	0.8	6.7[e])	8.3
3b	123	0.75	*ca.* 10000	1.2	23.0	24.0[g])	1.0
4b	123	1.5	10295	1.2	5.8	7.2[g])	1.2
5b[h])	123	4	8436	1.1	0.8	4.5[g])	5.6

[a]) K values are given by *Eqn. 3* ($[I]_0 = 0.044$M, $k_p = 2000$ l mol^{-1} s^{-1}, and $k_t = 2.0\ 10^8$ l mol^{-1} s^{-1} [25]), at $t_{50\%}$, for the polystyryl (PS) alkoxyamines **1a–PS**, **2a–PS**, **3a–PS**, **4a–PS**, and **5a–PS**. [b]) k_c were estimated with values given in columns 6 and 7 for **1a–PS**, **2a–PS**, **3a–PS**, **4a–PS**, and **5a–PS**. [c]) T, $t_{50\%}$, and *PDI* are from [12]. [d]) Not determined. [e]) From [11f]. [f]) T, $t_{50\%}$, M_n, and *PDI* are from [7c]. [g]) From [9a]. [h]) T 125°, $t_{50\%}$ 5–6 h, and $PDI = 1.03$ from [7c].

by *Guillaneuf et al.* [29] (k_c(**4a–PS**) $= 2.6 \cdot 10^5$ l mol^{-1} s^{-1} at room temperature) for the recombination of the polystyryl radical and **4a**.

$$K = \frac{k_d}{k_c} = \left(\frac{2 \ln 2}{3k_p}\right)^3 \cdot \frac{3k_t}{[I]_0 t_{50\%}^2} \tag{3}$$

All alkoxyamines **3b**, **4b**, and **5b** can be used to carry out an NMP experiment yielding controlled and living polystyrene. Moreover, alkoxyamine **3b** is the most efficient agent for NMP, *i.e.*, yields the shortest polymerization time (*Table 3*), and a low *PDI* (<1.3).

Conclusion. – Combining X-ray analysis and EPR spectroscopy, we showed that the phosphoryl group is a better H-bond acceptor than the nitroxide moiety. Moreover, we showed the importance of intramolecular H-bonding and of stabilizing electrostatic interactions on the value of k_d and on the fate of the NMP. Furthermore, we highlighted the potential of alkoxyamines containing a β-phosphorylated aminooxy fragment and releasing a nitroxide radical capable of intramolecular H-bonding as controller agents.

The authors thank *M. Giorgi* for having performed X-ray analysis and the University of Provence, ENSCM, CNRS, and *Arkema* for their financial support. *S. A.* and *C. L. M.* thank *Arkema* for their 3-years grant.

Experimental Part

General. Solvents for syntheses, copper bromide, copper metal, Et_3N, *N,N*-dimethylpyridin-4-amine (DMAP), alcohols, *N,N,N′,N′,N″*-pentamethyldiethylenetriamine (pmdien) and 2-bromo-2-methylpropanoyl bromide were purchased from *Aldrich* and used as received. Styrene and (*tert*-butyl)benzene were purchased from *Aldrich* and purified by conventional procedures [30]. Nitroxide radical **4a** (SG1) was kindly provided by *Arkema*. Nitroxide radical **5a** and alkoxyamines **4b** and **5b** were prepared following known procedures [7b][31]. TLC (reaction monitoring): silica gel plates (*60 F 240*, eluent AcOEt/pentane 1:1), detection by UV and phosphomolybdic acid. Column chromatography (CC): silica gel *60* (70–230 mesh, *Merck*), eluent AcOEt/pentane 3:1. NMR Spectra (performed in the 'Spectropôle', Marseille): *Avance-Bruker-300* spectrometer; ^{1}H at 300, ^{13}C at 75.48, and ^{31}P at 121.59 MHz; $CDCl_3$ solns.; δ in ppm rel. to $SiMe_4$ (internal ref.) for ^{1}H, to $CDCl_3$ (internal ref.) for ^{13}C, and to 85% H_3PO_4 soln. (external ref.) for ^{31}P, *J* in Hz. Elemental analyses were performed in the 'Spectropôle', Marseille.

1-(Diethoxyphosphoryl)-2,2-dimethylpropyl 2-Hydroxy-1,1-dimethylethyl Nitroxide (**3a**): At 10° and under N_2, 2-amino-2-methylpropan-1-ol (2.87 g, 33 mmol) was added dropwise to a soln. of pivalaldehyde (=2,2-dimethylpropanal; 2.6 g, 30 mmol). The mixture was heated up to 40° for 6 h, and the H_2O was removed. Molecular sieves were added, and the soln. was heated at 40° for 1 h. Diethylphosphonate (6.21 g, 45 mmol) was added at r.t., and the mixture was heated at 40° for 22 h. The mixture was poured in CH_2Cl_2 and the precipitate filtered off. The soln. was acidified with 5% HCl soln. (→ pH 3), and the soln. washed with CH_2Cl_2 (5×20 ml). The aq. layer was basified with $KHCO_3$ (→ pH 8) and then extracted with CH_2Cl_2 (2×20 ml), the org. layer dried ($MgSO_4$), and the solvent evaporated: amine (4.41 g, 50%). Colorless oil. ^{1}H-NMR ($CDCl_3$, 400 MHz): 0.91 (*s*, 3 H); 0.98 (*s*, 9 H); 1.07 (*s*, 3 H); 1.29 (*t*, *J*(H,H)=7.0, 3 H); 1.30 (*t*, *J*(H,H)=7.0, 3 H); 2.74 (*d*, *J*(H,P)=17.6, 1 H); 3.07 (*d*, *J*(H,H)=11.7, 1 H); 3.37 (*d*, *J*(H,H)=11.7, 1 H); 4.04–4.12 (*m*, 4 H); 5.05 (*s*, 1 H). ^{13}C-NMR ($CDCl_3$, 50.32 MHz): 16.15–16.34 (*m*, *Me*CH_2O); 22.87 (*s*, *Me*$_2$CCH_2OH); 26.96 (*s*, *Me*$_2$CCH_2OH); 27.80 (*d*, *J*(P,C)=5.9, *Me*$_3$C); 34.79 (*d*, *J*(P,C)=8,4, Me$_3$*C*); 54.55 (*s*, Me$_2$*C*CH_2OH); 58.82 (*d*, *J*(P,C)=141.9, CHP); 61.54 (*d*, *J*(C,P)=8.3, Me*C*H_2O); 62.34 (*d*, *J*(C,P)=8.3, Me*C*H_2O); 69.16 (*s*, *C*H_2OH). ^{31}P-NMR ($CDCl_3$, 40.53 MHz): 31.11.

A sat. aq. (20 ml) EtOH soln. of *Oxone* (24.5 g, 40 mmol) was added in small fractions to the amine (2.95 g, 10 mmol) and Na_2CO_3 (24.5 g, 60 mmol), at r.t. within 2 h under vigorous stirring. After completion, Et_2O (40 ml) was added, and the precipitate was filtered off. The Et_2O was removed, and the residue was taken up in heptane. The EtOH was removed by azeotropic distillation (EtOH/H_2O/heptane). The soln. was poured in H_2O (30 ml) and then extracted with CH_2Cl_2 (3×30 ml), the org. phase dried ($MgSO_4$), the solvent evaporated, and the residue subjected to CC (pentane/AcOEt 1:1): **3a** (2 g, 66%). Orange powder. M.p. 10–15°. Anal. calc.: C 50.29, H 9. 42, N 4. 51; found: C 50.31, H 9.40, N 4.47.

*Diethyl-{(1*RS*)-1-{(2-Hydroxy-1,1-dimethylethyl)[(1*SR*)-1-phenylethoxy]amino}-2,2-dimethylpropyl}phosphonate* ((*RS,SR*)-**3b**) *and* (*RR,SS*)-**3b**. To a degassed soln. of CuBr (0.35 g, 2.4 mmol) and copper (0.15 g, 2.4 mmol) in benzene, pmdien (0.66 g, 4.8 mmol) was added dropwise, and the soln. was kept under N_2 bubbling for another 10 min. Then, a degassed benzene soln. of **3a** (0.5 g, 1.6 mmol) and (1-bromoethyl)benzene (0.45 g, 2.4 mmol) was added, and the mixture was stirred for 2 days at r.t. under N_2.

Then, Et_2O (30 ml) was added and the solid filtered off. The org. layer was washed with H_2O until colorless, the org. layer dried ($MgSO_4$), the solvent evaporated to yield a colorless solid (65%). The two diastereoisomers were separated by CC (pentane/AcOEt 1:1). Anal. calc. for $C_{21}H_{38}NO_5P$: C 60.69, H 9.22, N 3.37; found: C 60.64, H 9.35, N 3.34.

*Data of (*RS,SR*)*-**3b**: M.p. 75°. ^{1}H-NMR (C_6D_6, 400 MHz): 0.80 (*t*, *J*(H,H) = 7.1, 3 H); 0.83 (*t*, *J*(H,H) = 7.1, 3 H); 1.15 (*s*, 3 H); 1.25 (*s*, 9 H); 1.26 (*s*, 3 H); 1.52 (*d*, *J*(H,H) = 6.7, 3 H); 3.51 (*m*, 5 H); 3.97 (*d*, *J*(H,P) = 26.8, 1 H); 4.11 (*d*, *J*(H,H) = 11.5, 1 H); 5.12 (*s*, 1 H); 5.26 (*q*, *J*(H,H) = 6.6, 1 H); 7.06 (*t*, *J*(H,H) = 7.3, 1 H); 7.17 (*m*, 2 H); 7.51 (*d*, *J*(H,H) = 7.4, 2 H). ^{13}C-NMR (C_6D_6, 100.64 MHz): 16.34 (*d*, *J*(C,P) = 6.1, *Me*CH_2O); 16.76 (*d*, *J*(C,P) = 6.3, *Me*CH_2O); 22.62 (*s*, *Me*$_2$$CCH_2OH$); 24.87 (*s*, PhCH(*Me*)O); 26.70 (*s*, *Me*$_2$$CCH_2OH$); 31.27 (*d*, *J*(C,P) = 6.5, *Me*$_3$C); 35.82 (*d*, *J*(C,P) = 3.0, Me$_3$*C*); 60.83 (*d*, *J*(C,P) = 7.9, Me*C*H_2O); 62.29 (*d*, *J*(C,P) = 6,3, Me*C*H_2O); 65.43 (*s*, Me$_2$*C*CH_2OH); 68.27 (*s*, CH_2OH); 70.28 (*d*, *J*(C,P) = 135.4, NCHP); 78.58 (*s*, Ph*C*H(Me)O); 127.3–128.7 (*m*, arom. CH); 128.7 (*s*, arom. C). ^{31}P-NMR (C_6D_6, 40.53 MHz): 26.86.

*Data of (*RR,SS*)*-**3b**: M.p. 81°. ^{1}H NMR (C_6D_6, 400 MHz): 0.81 (*s*, 3 H); 1.04–1.1 (*m*, 9 H); 1.31 (*s*, 9 H); 1.63 (*d*, *J*(H,H) = 6.7, 3 H); 3.23–3.27 (*m*, 1 H); 3.84 (*d*, *J*(H,P) = 26.6, 1 H); 3.94–4.01 (*m*, 4 H); 4.63 (*s*, 1 H); 5.00 (*m*, 1 H); 7.08 (*t*, *J*(H,H) = 5.3, 1 H); 7.15 (*m*, 2 H); 7.35 (*d*, *J*(H,H) = 6.1, 2 H). ^{13}C-NMR (C_6D_6, 100.64 MHz): 16.66 (*d*, *J*(C,P) = 6.2, *Me*CH_2O); 16.91 (*d*, *J*(C,P) = 5.9, *Me*CH_2O); 24.46 (*s*, *Me*$_2$$CCH_2OH$); 25.36 (*s*, PhCH(*Me*)O); 27.40 (*s*, *Me*$_2$$CCH_2OH$); 30.78 (*d*, *J*(C,P) = 5.1, *Me*$_3$C); 33.20 (*d*, *J*(C,P) = 4.2, Me$_3$*C*); 60.76 (*s*, Me$_2$*C*CH_2OH); 62.12 (*d*, *J*(C,P) = 5.9, Me*C*H_2O); 65.75 (*s*, Me*C*H_2O); 67.63 (*s*, CH_2OH); 70.18 (*d*, *J*(C,P) = 134.0, NCHP); 86.09 (*s*, Ph*C*H(Me)O); 127.25–128.93 (*m*, arom. CH); 146.13 (*s*, arom. C). ^{31}P-NMR (C_6D_6, 40.53 MHz): 27.51.

EPR Measurements. The EPR spectra were recorded on a *Bruker-EMX* spectrometer with an NMR gaussmeter for field calibration. The sample consisted of a thaw-freeze–thaw-cycles-deoxygenated (*tert*-butyl)benzene soln. (10^{-4} M) of **3a** or **4a**. The instrument settings were as follows: microwave power 20 mW, modulation amplitude 0.3 G, modulation frequency 100 kHz, scan time 20 s, 2 K data points.

Polymerization Experiments. Typically, a mixture of alkoxyamine **3b**, **4b**, or **5b** (0.036 mmol) and styrene (7.24 mmol) in a *Schlenk* flask was thoroughly purged with Ar. Then, bulk polymerization was conducted at 123°, under Ar and magnetic stirring. Samples were withdrawn under positive Ar purge and analyzed by size-exclusion chromatography (SEC) and ^{1}H-NMR. Molecular masses were determined by SEC calibrated with polystyrene standards. SEC was performed with a *Spectra-Physics-Instruments-SP8810* pump and a *Shodex-RIse-61* refractometer detector (eluant THF, 30°, 1 ml min^{-1}, two columns *PLgel Mixed-D*).

Computational Method. All calculations were performed with the Gaussian 03 molecular orbital package [32]. The geometry optimizations were carried out without constraints at the UB3LYP/6-

Table 4. *Crystal Data, Data Collection and Refinement for Nitroxide Radicals (*R*)- and (*S*)-***3a***[a])*

Crystal color, habit	colorless, prism	θ [°]	1–22.64
Crystal dimensions [mm]	0.4 × 0.4 × 0.3	μ [mm^{-1}]	0.175
Formula	$C_{13}H_{29}NO_5P$	T [K]	298
M_r	310.34	Measured reflections	12440
Crystal system	orthorhombic	Reflections with $I > 3bI$	2387
Space group	Pca_{21}	*Miller* indices:	$-13 \le h \le 0$
Cell parameters:			$-18 \le k \le 0$
a [Å]	12.3330(10)		$-18 \le l \le 0$
b [Å]	16.691(3)	Refinement on F	Constrained H-atom parameters
c [Å]	16.259(3)	R	0.135
V [Å^3]	3470.4(90)	wR	0.250
Z	8	Godness of fit S	3.77
D_x [Mg·m^{-3}]	1.25	Reflections	2531
Radiation	MoK_α	Parameters	360
Reflections for cell parameters	12440	$\Delta\sigma$ (max, min) [eÅ^{-3}]	0.70, −0.71

31++G(d,p) level of theory. Vibrational frequencies were calculated at the UB3LYP/6-31++G(d,p) level to determine the nature of the located stationary points. Frequency calculations were performed to confirm that the geometry was a minimum (zero imaginary frequency). The single-point energies were then calculated at the UB3LYP3/6-311++G(3df,3pd) level of theory. The optimized preferred conformation of the model compound was analyzed with the natural-bond-orbitals method [33], included in the Gaussian 03 package (NBO 3.1).

X-Ray Measurement. Experiments were performed on a *Bruker-Nonuis-KappaCCD* diffractometer with MoK_α source. All the data needed for the determination of the X-ray crystal structure are listed in *Table 4*.

REFERENCES

[1] D. H. Solomon, E. Rizzardo, P. Cacioli, US Pat. 4,581,429, 1986; Eur. Pat. Appl. 135280, 1985 (*Chem. Abstr.* **1985**, *102*, 221335q).

[2] M. K. Georges, R. P. N. Veregin, P. M. Kazmaier, G. K. Hamer, *Macromolecules* **1993**, *26*, 2987.

[3] C. J. Hawker, A. W. Bosman, E. Harth, *Chem. Rev.* **2001**, *101*, 3661 and references cited therein.

[4] D. Greszta, K. Matyjaszewski, *Macromolecules* **1996**, *29*, 7661 and ref. cit. therein.

[5] H. Fischer, *Chem. Rev.* **2001**, *101*, 3581 and ref. cit. therein; T. Fukuda, A. Goto, Y. Tsujii, in 'Handbook of Radical Polymerization', Eds. K. Matyjaszewski and Th. P. Davis, Wiley-Interscience, 2002, Chap. 9, pp. 407–462; P. Lacroix-Desmazes, J.-F. Lutz, B. Boutevin, *Macromol. Chem. Phys* **2000**, *201*, 662; P. Lacroix-Desmazes, J.-F. Lutz, F. Chauvin, R. Severac, B. Boutevin, *Macromolecules* **2001**, *34*, 8866; J.-F. Lutz, P. Lacroix-Desmazes, B. Boutevin, *Macromol. Rapid Commun.* **2001**, *22*, 189.

[6] 'Controlled Radical Polymerization', Ed. K. Matyjaszewski, American Chemical Society, Washington DC, 1998, Vol. 685; 'Controlled-Living Radical Polymerization: Progress in ATRP, NMP, and RAFT', Ed. K. Matyjaszewski, American Chemical Society, Washington, D.C., 2000, Vol. 768; K. Matyjaszewski, *Macromol. Symp.* **2001**, *174*, 51; C. J. Hawker, 'Handbook of Radical Polymerization', Eds. K. Matyjaszewski and Th. P. Davis, Wiley-Interscience, 2002, Chap. 9, pp. 463–522.

[7] a) G. Moad, E. Rizzardo, *Macromolecules* **1995**, *28*, 8722; b) S. Grimaldi, F. Le Moigne, J.-P. Finet, P. Tordo, P. Nicol, M. Plechot, Int. Pat. WO 96/24620, 1996; c) D. Benoit, V. Chaplinski, R. Braslau, C. J. Hawker, *J. Am.Chem. Soc.* **1999**, *121*, 3904; d) M.-O. Zink, A. Kramer, P. Nesvadba, *Macromolecules* **2000**, *33*, 8106; e) C. Le Mercier, S. Acerbis, D. Bertin, F. Chauvin, D. Gigmes, O. Guerret, M. Lansalot, S. Marque, F. Le Moigne, H. Fischer, P. Tordo, *Macromol. Symp.* **2002**, *182*, 225; f) J.-L. Couturier, O. Guerret, D. Gigmes, S. Marque, F. Chauvin, P.-E. Dufils, D. Bertin, P. Tordo, Pat. No. FR2843394, 2004, WO 2004014926; g) N. R. Cameron, C. A. Bacon, A. J. Reid, 'Advances in Controlled/Living Radical Polymerization', 'ACS Symposium Series', Ed. K. Matyjaszewski, American Chemical Society, Washington, D.C., 2003, Vol. 854, p. 452; h) E. Drockenmuller, J.-M. Catala, *Macromolecules* **2002**, *35*, 2461; i) Y. Miura, A. Ichikawa, H. Taniguchi, *Polymer* **2003**, *44*, 5187; j) T. Schulte, A. Studer, *Macromolecules* **2003**, *36*, 3078.

[8] F. Chauvin, P.-E. Dufils, D. Gigmes, Y. Guillaneuf, S. R. A. Marque, P. Tordo, D. Bertin, *Macromolecules* **2006**, *39*, 5238.

[9] a) S. Marque, C. Le Mercier, P. Tordo, H. Fischer, *Macromolecules* **2000**, *33*, 4403; b) P. Marsal, M. Roche, P. Tordo, P. de Sainte Claire, *J. Phys. Chem. A* **1999**, *103*, 2899.

[10] a) C. Le Mercier, J.-F. Lutz, S. Marque, F. Le Moigne, P. Tordo, P. Lacroix-Desmazes, B. Boutevin, J.-L. Couturier, O. Guerret, R. Martschke, J. Sobek, H. Fischer, in 'Controlled Radical Polymerization', 'ACS Symposium Series', Ed. K. Matyjaszewski, Washington, D.C., 2000, Vol. 768, p. 108; b) D. Bertin, D. Gigmes, C. Le Mercier, S. Marque, P. Tordo, *J. Org. Chem.* **2004**, *69*, 4925; c) D. Bertin, D. Gigmes, S. R. A. Marque, P. Tordo, *Macromolecules* **2005**, *38*, 2638; d) S. Marque, *J. Org. Chem.* **2003**, *68*, 7582.

[11] a) C. L. Moad, G. Moad, E. Rizzardo, S. H. Thang, *Macromolecules* **1996**, *29*, 7717; b) W. G. Skene, S. T. Belt, T. J. Connolly, P. Hahn, J. C. Scaiano, *Macromolecules* **1998**, *31*, 9103; c) M. V. Ciriano, H.-G. Korth, W. B. Van Scheppingen, P. Mulder, *J. Am. Chem. Soc.* **1999**, *121*, 6375; d) N. R. Cameron, A. J. Reid, P. Span, S. A. F. Bon, J. J. G. S. van Es, A. L. German, *Macromol. Chem.*

Phys. **2000**, *201*, 2510; e) A. Goto, T. Fukuda, *Macromol. Chem. Phys.* **2000**, *201*, 2138; f) S. Marque, H. Fischer, E. Baier, A. Studer, *J. Org. Chem.* **2001**, *66*, 1146; g) J.-F. Lutz, P. Lacroix-Desmazes, B. Boutevin, C. Le Mercier, D. Gigmes, D. Bertin, P. Tordo, *Polym. Prep. (ACS, Div. Polym. Chem.)* **2002**, *43*, 287.

[12] E. Harth, B. Van Horn, C. J. Hawker, *J. Chem. Soc., Chem. Commun.* **2001**, 823.

[13] M. Charton, *Top. Curr. Chem.* **1983**, *114*, 57.

[14] S. Grimaldi, D. Siri, J.-P. Finet, P. Tordo, *Acta Crystallogr., Sect. C: Cryst. Struct. Commun.* **1998**, *54*, 1712.

[15] D. L. Haire, V. M. Oehler, P. H. Krygsman, E. G. Janzen, *J. Org. Chem.* **1988**, *53*, 4535; D. L. Haire, Y. Kotake, E. G. Janzen, *Can. J. Chem.* **1988**, *65*, 1901; Y. Kotake, K. Kuwata, *Bull. Chem. Soc. Jpn.* **1982**, *55*, 3686; E. G. Janzen, J. I-P. Liu, *J. Magn. Reson.* **1973**, *9*, 510.

[16] N. Isaacs, 'Physical Organic Chemistry', 2nd edn., Longman, 1995.

[17] G. A. Jeffrey, W. Saenger, 'Hydrogen Bonding in Biological Structures', Springer-Verlag, Berlin–Heidelberg, 1994.

[18] C. M. Breneman, K. B. Wiberg, *J. Comput. Chem.* **1990**, *11*, 361.

[19] E. G. Janzen, 'Topics in Stereochemistry', Eds. E. G. Allinger and E. L. Eliel, Wiley-Interscience, New York, 1971, Vol. 6, p. 177.

[20] P. Tordo, M. Boyer, A. Friedmann, O. Santero, L. Pujol, *J. Phys. Chem.* **1978**, *82*, 1742; L. Dembrowski, J.-P. Finet, C. Fréjaville, F. Le Moigne, R. Maurin, A. Mercier, P. Pages, P. Stipa, P. Tordo, *Free Rad. Res. Commun.* **1993**, *19 Suppl.*, S23.

[21] F. Gerson, W. Huber, 'Electron Spin Resonance Spectrosocpy of Organic Radicals', Wiley-VCH, Weinheim, 2003.

[22] S. Grimaldi, Ph. D. Thesis, Université de Provence in Marseille, France, 1998.

[23] S. Acerbis, Ph. D. Thesis, Université de Provence in Marseille, France, 2002.

[24] G. Ananchenko, M. Souaille, H. Fischer, C. Le Mercier, P. Tordo, *J. Polym. Sci., Part A: Polym. Chem.* **2002***, 4,* 3264.

[25] S. Beuermann, M. Buback, *Progr. Polym. Sci.* **2002**, *27*, 191.

[26] D. Bertin, F. Chauvin, S. Marque, P. Tordo, *Macromolecules* **2002**, *35*, 10, 3790; O. Guerret, J.-L. Couturier, F. Chauvin, H. El-Bouazzy, D. Bertin, D. Gigmes, S. Marque, H. Fischer, P. Tordo 'ACS Symposium Series', American Chemical Society, Washington, D.C., 2003, Vol. 854, p. 412.

[27] J. Sobek, R. Martschke, H. Fischer, *J. Am. Chem. Soc.* **2001**, *123*, 2849.

[28] A. L. J. Beckwith, V. W. Bowry, K. U. Ingold, *J. Am. Chem. Soc.* **1992**, *114*, 4983.

[29] Y. Guillaneuf, D. Bertin, P. Castignolles, B. Charleux, *Macromolecules* **2005**, *38*, 4638.

[30] D. D. Perrin, W. L. F. Armarego, 'Purification of Laboratory Chemicals', 3rd edn., Pergamon Press.

[31] K. Matyjaszewski, B. E. Woodworth, X. Zhang; S. Gaynor, Z. Metzner, *Macromolecules* **1998**, *31*, 5955.

[32] M. J. Frisch, G. W. Trucks, H. B. Schlegel, G. E. Scuseria, M. A. Robb, J. R. Cheeseman, J. A. Montgomery Jr., T. Vreven, K. N. Kudin, J. C. Burant, J. M. Millam, S. S. Iyengar, J. Tomasi, V. Barone, B. Mennucci, M. Cossi, G. Scalmani, N. Rega, G. A. Petersson, H. Nakatsuji, M. Hada, M. Ehara, K. Toyota, R. Fukuda, J. Hasegawa, M. Ishida, T. Nakajima, Y. Honda, O. Kitao, H. Nakai, M. Klene, X. Li, J. E. Knox, H. P. Hratchian, J. B. Cross, C. Adamo, J. Jaramillo, R. Gomperts, R. E. Stratmann, O. Yazyev, A. J. Austin, R. Cammi, C. Pomelli, J. W. Ochterski, P. Y. Ayala, K. Morokuma, G. A. Voth, P. Salvador, J. J. Dannenberg, V. G. Zakrzewski, S. Dapprich, A. D. Daniels, M. C. Strain, O. Farkas, D. K. Malick, A. D. Rabuck, K. Raghavachari, J. B. Foresman, J. V. Ortiz, Q. Cui, A. G. Baboul, S. Clifford, J. Cioslowski, B. B. Stefanov, G. Liu, A. Liashenko, P. Piskorz, I. Komaromi, R. L. Martin, D. J. Fox, T. Keith, M. A. Al-Laham, C. Y. Peng, A. Nanayakkara, M. Challacombe, P. M. W. Gill, B. Johnson, W. Chen, M. W. Wong, C. Gonzalez, J. A. Pople, 'Gaussian 03, Revision C.02', *Gaussian. Inc.*, Wallingford CT, 2004.

[33] A. E. Reed, L. A. Curtiss, F. Weinhold, *Chem. Rev.* **1988**, *88*, 899.

Received February 15, 2006